



A Journal of the Gesellschaft Deutscher Chemiker

Angewandte Chemie

GDCh

International Edition

www.angewandte.org

Accepted Article

Title: Artificial light-harvesting complexes enable Rieske oxygenase-catalyzed hydroxylations in non-photosynthetic cells

Authors: Fatma Feyza Özgen, Michael Ernst Runda, Bastien O. Burek, Peter Wied, Jonathan Z. Bloh, Robert Kourist, and Sandy Schmidt

This manuscript has been accepted after peer review and appears as an Accepted Article online prior to editing, proofing, and formal publication of the final Version of Record (VoR). This work is currently citable by using the Digital Object Identifier (DOI) given below. The VoR will be published online in Early View as soon as possible and may be different to this Accepted Article as a result of editing. Readers should obtain the VoR from the journal website shown below when it is published to ensure accuracy of information. The authors are responsible for the content of this Accepted Article.

To be cited as: *Angew. Chem. Int. Ed.* 10.1002/anie.201914519
Angew. Chem. 10.1002/ange.201914519

Link to VoR: <http://dx.doi.org/10.1002/anie.201914519>
<http://dx.doi.org/10.1002/ange.201914519>

COMMUNICATION

Artificial light-harvesting complexes enable Rieske oxygenase-catalyzed hydroxylations in non-photosynthetic cells

F. Feyza Özgen,^[a] Michael E. Runda,^[a] Bastien O. Burek,^[b] Peter Wied,^[a] Jonathan Z. Bloh,^[b] Robert Kourist,^[a] and Sandy Schmidt*^[a]

Abstract: In this study, we coupled a well-established whole-cell system based on *E. coli* via light-harvesting complexes to Rieske oxygenase (RO)-catalyzed hydroxylations *in vivo*. Although these enzymes represent very promising biocatalysts, their practical applicability is hampered by their dependency on NAD(P)H as well as their multi-component nature and intrinsic instability in cell-free systems. In order to explore the boundaries of *E. coli* as chassis for artificial photosynthesis, and due to the reported instability of ROs, we used these challenging enzymes as model system. The light-driven approach relies on light-harvesting complexes such as eosin Y, 5(6)-carboxyeosin or rose bengal and sacrificial electron donors (EDTA, MOPS and MES) that were easily up-taken by the cells. The obtained product formations of up to 1.3 g/L and rates of up to 1.6 mM/h demonstrate that this is a comparable approach to typical whole-cell transformations in *E. coli*. The applicability of this photocatalytic synthesis has been demonstrated and represents the first example of a photo-induced RO system.

Nature's creativity in developing solutions for C-H-bond functionalization reactions like hydroxylations at activated or non-activated C-H-bonds is remarkably shown by an expansive list of metal-dependent enzymes.^[1,2] These enzymes, like the Rieske non-heme iron oxygenases (ROs) are able to activate molecular oxygen in order to generate reactive oxygen species capable of hydroxylating alkyl substrates, but also to promote further oxidative transformations.^[3–11] For many of these reactions no 'classical' chemical counterpart is known. Due to their dependency on complex electron transport chains^[12] as well as to provide an efficient *in situ* cofactor regeneration, the majority of synthetic applications of ROs relies on recombinant whole-cell catalysts. Generally, for such reactions various concepts have been developed that rely on electron supply *via* the metabolism of living heterotrophic cells.^[13–15] In synthetic applications, the nicotinamide cofactors are recycled by using energy-rich organic molecules as electron donors. In most cases, only a small fraction of the electrons provided by these sacrificial co-substrates is utilized, resulting in a poor atom efficiency.^[14] Moreover, when glucose is supplied as sacrificial substrate for the recycling of

NADPH, the often-used glucose dehydrogenase utilizes only a part of the electron pairs from each glucose molecule. In order to solve this challenge, many alternative solutions are currently under consideration.^[16–18] Next to linking photochemistry to enzymes *in vitro* for cofactor regeneration,^[18–24] autotrophic and chemolithoautotrophic organisms have recently received attention as they are capable of utilizing inorganic compounds as electron donors.^[25–29] Light-driven whole-cell reactions in cyanobacteria show the same reaction rates as *E. coli*.^[26,27,29] Yet, the strong absorption of the photosynthetic apparatus lead to self-shading of the cells at high densities, thus resulting in a low light utilization and a reduced photosynthetic activity.^[30] On the other hand, introducing artificial photosynthesis in heterotrophic bacteria such as *E. coli* offers the advantage of utilizing a genetically easy-to-manipulate organism along with the capability of producing high amounts of soluble protein within the cells. Additionally, these systems are less prone to the inhibiting effects of self-shading at high cell densities. Currently reported artificial light-driven approaches in heterotrophs comprise the use of inorganic-bio hybrid systems and the coupling of organic photosensitizers to biotransformations *in vivo*.^[31,32] One of the earliest examples of a whole-cell reaction was reported using recombinant *E. coli* coupled to photocatalytic H₂ production *via* an extracellular photosensitizer (TiO₂) and methyl viologen as electron mediator.^[31] Similarly, the light-driven H₂ evolution and C=C or C=O bond hydrogenation by *Shewanella oneidensis* using methyl viologen was shown.^[33] These are interesting systems, however, the toxicity of methyl viologen is well known, thus hampering large-scale applications. A direct and perhaps the most applicable approach has been reported by Park and coworkers.^[32] This light-driven catalysis is based on *in vivo* photoreduction of a P450 by using different fluorescent dyes and sacrificial electron donors.^[32] Although operating at low product concentrations, it represents a highly promising system for the challenging multi-component ROs since these enzymes usually exhibit high catalytic activities despite low expression levels, and thus a high potential for artificial photosynthesis approaches in *E. coli* (Figure 1).

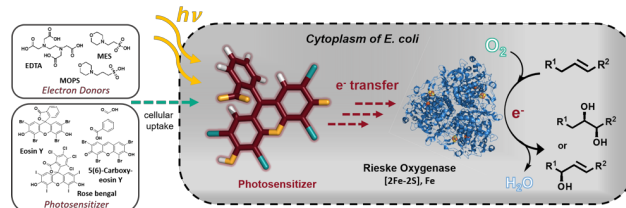


Figure 1. *In vivo* photoactivation of a Rieske non-heme iron oxygenase by an artificial light-harvesting complex. The catalytic turnover of the oxygenase-component is mediated by the excited photosensitizer that transfers electrons from the sacrificial electron donor to the oxygenase within the cytoplasm of *E. coli*.

[a] Fatma Feyza Özgen, MSc; Michael Ernst Runda, BSc; Dipl. Ing. Peter Wied; Prof. Dr. Robert Kourist; Dr. Sandy Schmidt
Institute of Molecular Biotechnology
Graz University of Technology
Petersgasse 14/1, 8010 Graz, Austria
E-mail: s.schmidt@tugraz.at

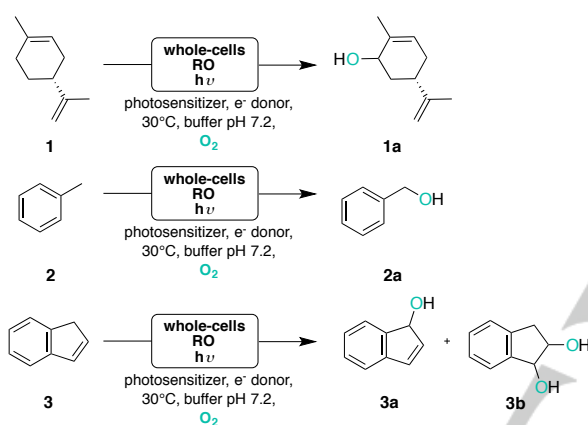
[b] Bastien O. Burek, MSc; Dr. Jonathan Z. Bloh
DECHEMA-Forschungsinstitut
Theodor-Huuss-Allee 25, 60486 Frankfurt am Main, Germany

[+] These authors contributed equally to this work.
Supporting information for this article is given via a link at the end of the document.

COMMUNICATION

Herein, we demonstrate the general feasibility of this light-induced approach together with a characterization of the crucial parameters determining the catalytic efficiencies of the light-driven *in vivo* enzymatic reaction.

We explored eosin Y (2,4,5,7-tetrabromofluorescein, EY) and its xanthene derivatives as well as safranin O (SO) as efficient photosensitizers to drive RO-catalyzed hydroxylation reactions under illumination with LED or fluorescent lamps. As electron donors, either 3-(N-morpholino)propane-sulfonic acid (MOPS), 2-(N-morpholino)ethanesulfonic acid (MES) or ethylenediaminetetraacetic acid (EDTA) have been investigated.^[23] In this way, the successive transfer of electrons reduces the catalytic iron and drives the conversion of (*R*)-limonene **1** into (1*R*,5*S*)-carveol **1a**, toluene **2** into benzyl alcohol **2a** or indene **3** to 1-indenol **3a** and *cis*- or *trans*-1,2-indandiol **3b** by the ROs under visible light irradiation and without the need of NAD(P)H as redox partner (Scheme 1).



Scheme 1. Light-driven whole-cell oxyfunctionalization reactions catalyzed by CDO or NDO, respectively.

We have chosen cumene dioxygenase (CDO, from *Pseudomonas fluorescens* IP01) and naphthalene dioxygenase (NDO, from *Pseudomonas* sp. NCIB 9816-4) as model enzymes (Figure S1, Tables S1-S7) since both enzymes have been extensively studied for a long time and many redesigned variants have been investigated. We became particularly interested in two variants of CDO and NDO, who have been engineered toward the asymmetric dihydroxylation of olefins. CDO variant M232A converts **1** almost exclusively to **1a** (*ee* > 98%),^[34] whereas NDO variant H295A shows a different ratio between allylic monohydroxylation and *cis*-dihydroxylation for several substituted arenes.^[35] First, we investigated the expression of the whole RO system under different culture conditions (SDS-PAGE, Figure S2) and confirmed the RO activity by an agar plate assay based on indigo formation (Figure S3, S4) and could identify significant activity toward indole.^[36] To identify the cell density leading to the highest product formation catalyzed by CDO expressed under different culture conditions, biotransformations supplemented with glucose (20 mM) and **1** (10 mM) as substrate have been performed under dark conditions (Table S8). As expected, CDO-containing whole cells (100 g_{WCW}/L) expressed in TB medium at 30°C gave the highest activity for **1** and the product **1a** was obtained with an *ee* of > 99% (Figure S5). The obtained product

concentrations of **1a** and **2a** were lower than previously reported,^[34] which we mostly contribute to a different expression protocol (19 hours instead of 2 hours) and a lower cell density (100 g_{WCW}/L instead of 200 g_{WCW}/L) than previously reported.^[34] However, we first investigated the light-driven system by using CDO-containing whole-cells at 100 g_{WCW}/L in order to avoid self-shading at too high cell densities and used cells expressed under the conditions mentioned above (19 hours).

We became interested in different photosensitizer / electron donor combinations to drive the light-driven whole-cell hydroxylation catalyzed by the ROs (Figures S6-S12, Table 1, Table S9 and 10).

Table 1. Photobiocatalytic hydroxylation of (*R*)-limonene **1**, toluene **2** and indene **3** catalyzed by CDO M232A and NDO H295A, respectively, under dark and light conditions.

Enzyme	Reaction conditions	Substrate	Product		Whole-cell activity ^[c] mU/g _{WCW}	
			Conc. [mM] ^[a]	<i>de</i> or <i>dr</i> ^[b] [%]		
CDO M232A	dark / glucose		1.1 ± 0.1	> 99	8.0	
	dark / CE / MES		0.1 ± 0.04		n.d.	
	light / CE / MES		0.4 ± 0.05		2.5	
Empty vector	light / CE / MES		0	n.d.	n.d.	
NDO H295A	dark / glucose		0.6 ± 0.02	n.a.	8.8	
	dark / CE / MES		0		n.d.	
	light / CE / MES		0.2 ± 0.01		2.8	
Empty vector	light / CE / MES		0	n.d.	n.d.	
CDO M232A	dark / glucose		4.8 ± 0.8	100 : 0	n.d.	
	dark / CE / MES		1.5 ± 0.2		100 : 0	n.d.
	light / CE / MES		8.3 ± 0.08		90 : 10	124
NDO H295A	dark / glucose		2.3 ± 0.17	100 : 0	n.d.	
	dark / CE / MES		0.5 ± 0.03		n.a.	n.d.
	light / CE / MES		8.5 ± 0.4		86 : 14	107
Empty vector	light / CE / MES		0.7 ± 0.2	18 : 82	n.d.	

Reaction conditions dark: [substrate] = 10 mM, [glucose] = 20 mM, [whole cells] = 100 g_{WCW}/L (*E. coli* JM109 (DE3)_{pDTG141_NDO H295A or *E. coli* JM109_{pCDOv1_CDO M232A}), sodium phosphate buffer (pH 7.2, 50 mM), 24 hours. Reaction conditions light: [substrate] = 10 mM, [whole cells] = 100 g_{WCW}/L (*E. coli* JM109 (DE3)_{pDTG141_NDO H295A or *E. coli* JM109_{pCDOv1_CDO M232A}), MES buffer (50 mM), white light illumination (max. 112 μE L⁻¹ s⁻¹) 24 hours; n.a. not applicable; n.d. not determined. ^[a] For **3**, product concentrations refer to the sum of **3a** and **3b**; ^[b] Diastereomeric ratio *cis:trans-3b* has been determined after 4-6 hours of reaction; ^[c] Determined from the linear range of product formation determined from the kinetic profiles for each reaction (Figures S20-S25).}}

We first chose MES since it has been successfully used as efficient electron donor previously,^[37] is non-toxic and can be up taken by *E. coli* cells.^[38,39] The *E. coli* strain herein used is lacking a natural uptake system for flavins,^[41] thus we decided to choose a PS that can easily enter the cells^[32] while showing similar redox properties such as flavins. 5(6)-carboxyeosin (CE) has been chosen first since it possesses excellent photosensitizer properties (Figure S8) with an *E*_{Redox} of -1.06 V, which is similar to the *E*_{Redox} of proflavine.^[40] Performing the photoenzymatic

COMMUNICATION

hydroxylation of **1** and **2** with 50 mM MES and 100 μM 5(6)-carboxyeosin (CE) at a cell density of 100 $\text{g}_{\text{WCW}}/\text{L}$ resulted in a smooth formation of the desired products **1a** (up to $\approx 360 \mu\text{M}$ in 24 hours) and **2a** (up to $\approx 200 \mu\text{M}$ in 24 hours) under illumination with white light. Nonetheless, the obtained concentrations of **1a** and **2a** always remained low ($\leq 360 \mu\text{M}$, Table 1). Due to the known toxicity of **1** as well as **1a** on whole-cells, we turned our attention toward indene **3** as typical substrate for ROs. In a next set of experiments, we investigated the same photosensitizer/electron donor combination for both model enzymes (Table 1) and were pleased to find that conversions of up to 85% were achieved with **3**. Since **3** was the most promising substrate to in-depth characterize our light-driven system, we turned our attention to the investigation of further photosensitizer/electron donor combinations. We investigated EY, rose bengal (RB) and CE with EDTA, but also with MOPS and MES as sacrificial electron donors that can be up taken by cells (Table 2).^[39,40,43] The electron donor can constitute an obstacle in this photobiocatalytic setup,^[23] as EDTA may suffer *e.g.* from incompatibility with the RO due to its ability to sequester the Fe^{3+} ion which is located in the active site of the oxygenase. However, we did not see any activity loss of NDO H295A and CDO M232A in dark reactions supplemented with EDTA (Figure S13) nor any toxicity effects of MES/MOPS on the cells (Figure S14). Moreover, when performing the light-driven hydroxylations with lysed cells, product formations of only 5.6 mM compared to 8.5 mM with whole cells were achieved (Table S11), indicating that the cells do not suffer from the electron donors or decomposition products thereof. The obtained product formations with **3** as substrate are summarized in Table 2. Reactions supplemented with EDTA led in general to a lower product formation compared to reactions with MOPS and MES. However, also with EDTA product concentrations of up to 7.5 mM could be achieved, leading to the assumption that EDTA is not sequestering the catalytic iron ion from the enzyme's active site. Moreover, we were pleased to find that the utilization of **3** as substrate boosted the product formation in the mM range, leading to a conversion of up to $>85\%$ within 24 hours when using CE in combination with MES (Table 1 and 2). The determination of the incident photon flux density (Figure S11B) revealed that the light intensity at each position of the light reactor varies in a range between 32-112 $\mu\text{E L}^{-1} \text{s}^{-1}$, which causes a light-intensity-dependent photochemical background reaction. This photochemical background reaction is only observed when **3** is used as substrate and leads to the accumulation of *trans*-**3b** within 6-20 hours of reaction (Figure S15-S17). Moreover, 1-indanone formation has been observed, which we attribute to an isomerization reaction of **3a** (Table S12). To determine the incident photon flux, chemical actinometry was performed using the well-described ferrioxalate actinometer (Table 2 and Table S10).^[44] Although the cell suspension showed strong scattering and optical absorption by other cell or solution components, we were able to estimate quantum yields (QY, Table S10). Additionally, apparent quantum yields (AQY) were calculated as the ratio of two times the observed product formation rate to the incident photon flux, as two photons are required per turnover (Table 2). Admittedly, the given AQYs are lower than the typical values achieved in photochemical reactions, however, these values lay a promising foundation for further optimization of this artificial photosynthetic systems.

To investigate whether the observed product formation was strictly light-dependent and only proceeded through the electron transfer mediated by the photosensitizer, we conducted control reactions with an empty vector control, but performed in light and dark with and without electron donor (Figure 2A, Figure S19).

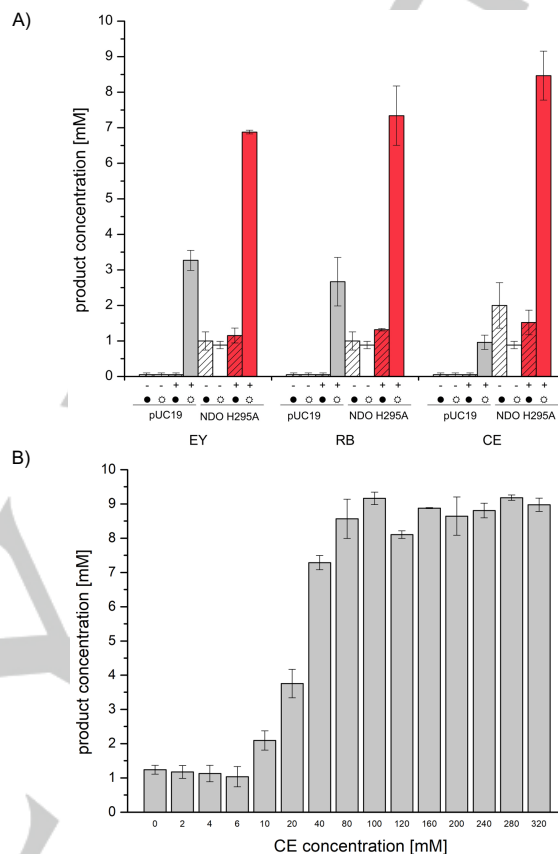
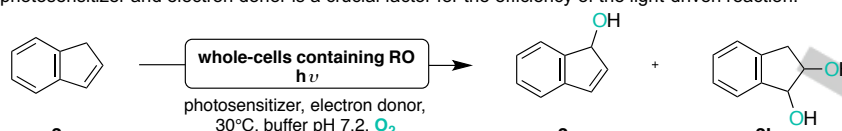


Figure 2. A) Performed control reactions using NDO H295A under light (○) and dark (●) conditions with (+) or without (-) 100 μM EY, RB or CE in the presence of NDO H295A (red bars) or with an empty vector control (grey bars) in 50 mM MOPS. Values for the empty vector control were the highest that have been achieved when the max. light intensity of 112 $\mu\text{E L}^{-1} \text{s}^{-1}$ were applied. B) Effect of photosensitizer concentration on product yield. Different concentrations of CE used in combination with MES as electron donor in the light-driven whole-cell hydroxylation reaction employing NDO H295A. Reaction conditions: 0-320 μM photosensitizer, 10 mM **3**, 50 mM MES, 100 $\text{g}_{\text{WCW}}/\text{L}$ whole cells (*E. coli* JM109 (DE3)_pDTG141_NDO H295A, 19h expression), 50 mM MES, white light (max. 112 $\mu\text{E L}^{-1} \text{s}^{-1}$), 30°C, 140 rpm.

Indeed, the obtained product formations with the empty vector controls were much lower under dark and light conditions. We attribute the turnover in the dark to the production of carbohydrates, which under “famine conditions” were consumed to regenerate NAD(P)H.^[26,27,44,45] However, under light conditions a photochemical background reaction has been observed, which varies depending on the applied light intensity between 0.15 to 3.5 mM and depending on the applied photosensitizer/electron donor combination (Figure 2A, Figure S19). The background reaction contributed up to 12% of total product formation when using CE/MOPS and 35% when using RB/MOPS (Figure 2A), indicating that the photochemical background reaction depends on the photosensitizer.

COMMUNICATION

Table 2. The combination of photosensitizer and electron donor is a crucial factor for the efficiency of the light-driven reaction.


Enzyme	Photosensitizer, electron donor	Products			Whole-cell activity		Apparent quantum yield [%]
		Maximum concentration [mM] ^[a]	Diastereomeric ratio <i>cis</i> : <i>trans</i> - 3b [%] ^[b]	Distribution 3a : 3b [%] ^[c]	Specific activity ^[d] [mU/gwcw]	Productivity [mM/h]	
CDO M232A	EY/EDTA	3.7 ± 0.4	100 : 0	3 : 97	29	0.18	0.09
	EY / MOPS	6.8 ± 0.03	100 : 0	0 : 100	21	0.13	0.06
	EY / MES	4.7 ± 0.2	100 : 0	4 : 96	41	0.25	0.12
	RB / EDTA	6.8 ± 0.3	96 : 4	4 : 96	265	1.59	0.78
	RB / MOPS	7.3 ± 0.6	95 : 5	4 : 96	156	0.94	0.46
	RB / MES	5.8 ± 0.4	95 : 5	3 : 97	275	1.65	0.81
	CE / EDTA	4.0 ± 0.01	94 : 6	2 : 98	43	0.26	0.13
	CE / MOPS	8.6 ± 0.6	88 : 12	0 : 100	102	0.61	0.30
	CE / MES	8.3 ± 0.08	90 : 10	0 : 100	124	0.75	0.37
NDO H295A	EY/EDTA	4.7 ± 0.2	96 : 4	4 : 96	47	0.23	0.11
	EY / MOPS	7.7 ± 0.4	83 : 17	2 : 98	61	0.37	0.18
	EY / MES	7.4 ± 0.3	86 : 14	4 : 96	87	0.52	0.26
	RB / EDTA	7.5 ± 1.0	97 : 3	0 : 100	53	0.32	0.16
	RB / MOPS	7.5 ± 1.2	95 : 5	2 : 98	148	0.89	0.44
	RB / MES	7.9 ± 0.6	97 : 3	3 : 97	79	0.45	0.22
	CE / EDTA	5.5 ± 0.5	94 : 6	6 : 94	50	0.30	0.15
	CE / MOPS	7.3 ± 0.4	95 : 5	18 : 82	143	0.86	0.42
	CE / MES	8.5 ± 0.4	86 : 14	0 : 100	107	0.64	0.32

Reaction conditions: [**3**] = 10 mM; [whole cells] = 100 gwcw/L (*E. coli* JM109 (DE3)_pDTG141_NDO H295A or *E. coli* JM109_pCDOv1_CDO M232A); sodium phosphate buffer (pH 7.2, 50 mM) when using 25 mM EDTA, otherwise 50 mM MES/MOPS buffer; white light illumination (max. 112 $\mu\text{E L}^{-1} \text{s}^{-1}$). ^[a] Sum of **3a** and **3b**; time points for determination were chosen at max. product concentration during the time course of the reaction; ^[b] The diastereomeric ratio has been determined after 4-6 hours of reaction. ^[c] Determined after 24 hours. ^[d] Determined from the linear range of product formation determined from the kinetic profiles for each reaction (Figures S19-S24).

This capability seems to be limited by the applied light intensity, since the overall background reaction remained low in all cases (< 0.5 mM) when lower light intensities were used, thus confirming that the reaction is truly light-driven.

Additionally, we investigated the influence of the photosensitizer (Figure 2B) and electron donor concentration, as well as the cell densities (Figure S18) on the efficiency of the photocatalytic activation of NDO H295A. Under light illumination, the RO catalyzed hydroxylation of **3** is most efficient when CE concentrations of 80 to 100 μM were used. Between 10 μM and 80 μM of CE, an increase in product formation is observed (Figure 2B). However, when using >100 μM of CE, no further increase can be seen, i.e. that above 100 μM CE either the concentration is not limited or the transport of the photosensitizer inside the cells is hampered (Figure 2B). However, we observed photobleaching over time. When additional 100 μM of CE were added to the light-driven hydroxylation, the product formation accelerates again, and after 6 hours after adding additional CE already 7.2 mM of product has been formed in contrast to only 3 mM without adding additional CE (Figure 3A).

We further investigated the effect of increasing cell densities on the efficiency of the light-driven hydroxylation reaction (Figure S18). When increasing the cell density as well as the electron

donor concentration (CE constant), it can be seen that the product formation is influenced by the concentration of the electron donor when the cell density is higher, because more photo-induced electrons are transferred to the enzyme. However, the system seems to be limited by the applied light intensities (max. 112 $\mu\text{E L}^{-1} \text{s}^{-1}$), i.e. that from a certain cell density on, the product concentration is not "controlled" anymore by the concentration of the electron donor, and at that point the light intensity in the system becomes the limiting factor.

Light intensity plays a crucial role on the efficiency of the light-driven catalysis, and influences the extend of the photochemical background reaction. When reducing the light intensity by 75% (Figure S10B), the obtained product concentrations decreased by only 20%. Finally, we followed the light-driven reaction in a time-course experiment over 24 hours under optimized conditions (Figure 3B). The product formation proceeds smoothly within 24 hours of reaction, however, in case of NDO H295A/MES/CE and CDO M232A/MOPS/CE no significant product increase is observed after 20 hours. Noteworthy, when using SO in combination with MOPS or EDTA, obtained product concentrations remained always lower compared to other photosensitizer/electron donor combinations.

COMMUNICATION

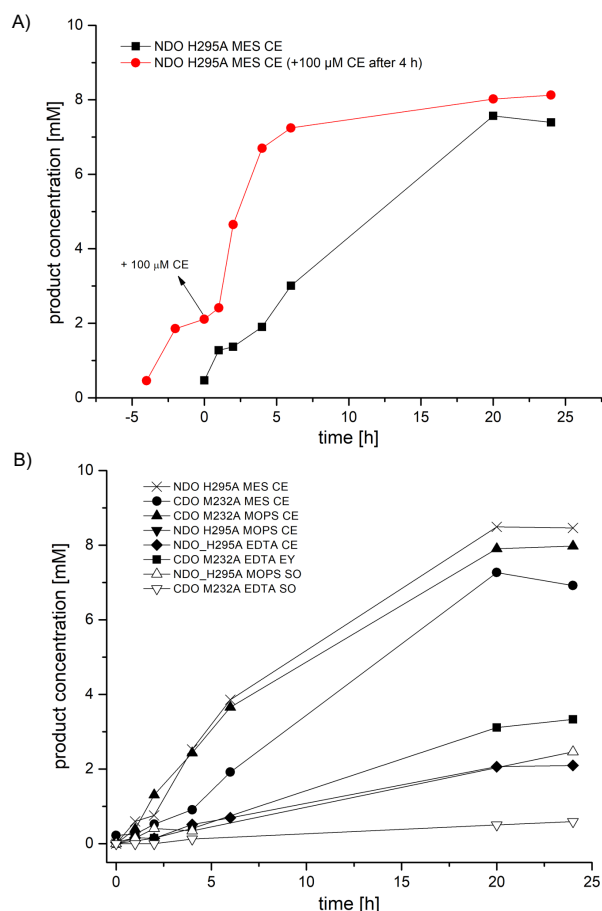


Figure 3. A) Effect of photobleaching of CE on the time course of the light-driven hydroxylation catalysed by NDO H295A. The red curve visualizes the addition of again 100 μM CE after 4 h of biotransformation, whereas the black curve shows the light-driven biotransformation without adding additional CE. **B)** Kinetic profile obtained for the light-driven whole-cell hydroxylation reaction employing CDO M232A and NDO H295A with SO, CE and EY in combination with either EDTA, MOPS or MES as electron donors. Reaction conditions: 100 μM photosensitizer, 10 mM **3**, 25 mM EDTA or 50 mM MOPS/MES, in A) 25–300 $\text{g}_{\text{WCW}}/\text{L}$ and in B) 100 $\text{g}_{\text{WCW}}/\text{L}$ whole cells (*E. coli* JM109 (DE3)_pDTG141_NDO H295A or *E. coli* JM109_pCDOv1_CDO M232A, 19h expression), white light (max. 112 $\mu\text{E L}^{-1} \text{s}^{-1}$), 30°C, 140 rpm, 24 hours.

To conclude, we have shown the photo-activation of two different ROs in an *E. coli*-based whole-cell system by coupling light-harvesting complexes to hydroxylation reactions *in vivo*. This was successfully conducted by using several photosensitizers for the bioconversion of three different substrates, hence representing the first example of photo-induced RO systems. Particularly for challenging multi-component oxygenases, this system offers the advantage of relying on the well-studied genetic toolbox of *E. coli* as host, thereby facilitating a broad applicability of light-driven artificial photosynthesis. The obtained product formations of up to 1.3 g/L and rates of up to 1.6 mM/h demonstrate that competitive productivities compared to cyanobacteria were achieved.^[28] The coupling of artificial light-harvesting complexes to enzymes inside cells provides a versatile route to accessing diverse and selective visible-light-driven chemical syntheses especially when unstable or multi-component enzymes are used.

Experimental Section

All experimental details can be found in the Supporting Information.

Acknowledgements

This project has received funding from the European Union's Horizon 2020 research and innovation program under the Marie Skłodowska-Curie grant agreement No. 764920. We thank Prof. Dr. Rebecca Parales for providing us with the vector pDTG141 harboring the NDO genes and Prof. Dr. Hideaki Nojiri for plasmid pIP107D harboring the CDO genes.

Keywords: biocatalysis • oxyfunctionalization • photocatalysis • photoinduced electron transfer • Rieske dioxygenases

- [1] J. C. Lewis, P. S. Coelho, F. H. Arnold, *Chem. Soc. Rev.* **2011**, *40*, 2003–2021.
- [2] J. Dong, E. Fernández-Fueyo, F. Hollmann, C. E. Paul, M. Pesic, S. Schmidt, Y. Wang, S. Younes, W. Zhang, *Angew. Chem. Int. Ed.* **2018**, *57*, 9238–9261; *Angew. Chem.* **2018**, *130*, 9380–9404.
- [3] D. J. Ferraro, L. Gakhar, S. Ramaswamy, *Biochem. Biophys. Res. Commun.* **2005**, *338*, 175–190.
- [4] S. M. Barry, G. L. Challis, *ACS Catal.* **2013**, *3*, 2362–2370.
- [5] W. A. Tan, R. E. Parales, *Green Biocatal.* **2016**, 457–471.
- [6] W. K. Dawson, R. Jono, T. Terada, K. Shimizu, *PLoS One* **2016**, *11*, e0162031.
- [7] R. E. Parales, S. M. Resnick, in *Biodegrad. Bioremediation* (Eds.: A. Singh, O.P. Ward), Springer Berlin Heidelberg, Berlin, Heidelberg, **2004**, 175–195.
- [8] R. E. Parales, S. M. Resnick, C. L. Yu, D. R. Boyd, N. D. Sharma, D. T. Gibson, *J. Bacteriol.* **2000**, *182*, 5495–5504.
- [9] O. Kweon, S. J. Kim, S. Baek, J. C. Chae, M. D. Adjei, D. H. Baek, Y. C. Kim, C. E. Cerniglia, *BMC Biochem* **2008**, *9*, 4268–4273.
- [10] F. F. Özgen, S. Schmidt, in *Biocatalysis* (Eds.: Q. Husain, M.F. Ullah), Springer International Publishing, Cham, **2019**, 57–82.
- [11] D. J. Ferraro, A. Okerlund, E. Brown, S. Ramaswamy, *IUCrJ* **2017**, *4*, 648–656.
- [12] Y. Ashikawa, Z. Fujimoto, H. Noguchi, H. Habe, T. Omori, H. Yamane, H. Nojiri, *Structure* **2006**, *14*, 1779–1789.
- [13] C. Schmidt-Dannert, F. Lopez-Gallego, *Microb. Biotechnol.* **2016**, *9*, 601–609.
- [14] L. M. Blank, B. E. Ebert, K. Buehler, B. Bühler, *Antioxid. Redox Signaling* **2010**, *13*, 349–394.
- [15] V. Uppada, S. Bhaduri, S. B. Noronha, *Curr. Sci.* **2014**, *106*, 946.
- [16] J. Kim, C. B. Park, *Curr. Opin. Chem. Biol.* **2019**, *49*, 122–129.
- [17] B. O. Burek, S. Bormann, F. Hollmann, J. Z. Bloh, D. Holtmann, *Green Chem.* **2019**, *21*, 3232–3249.
- [18] W. Zhang, F. Hollmann, *Chem. Commun.* **2018**, *54*, 7281–7289.
- [19] S. H. Lee, D. S. Choi, S. K. Kuk, C. B. Park, *Angew. Chem. Int. Ed.* **2018**, *57*, 7958–7985.
- [20] T. Gulder, C. J. Seel, *ChemBioChem* **2019**, *20*, 1871.
- [21] L. Schermund, V. Jurkaš, F. F. Özgen, G. D. Barone, H. C. Büchschütz, C. K. Winkler, S. Schmidt, R. Kourist, W. Kroutil, *ACS Catal.* **2019**, 4115–4144.
- [22] D. Adam, L. Bösche, L. Castañeda-Losada, M. Winkler, U. P. Apfel, T. Happe, *ChemSusChem* **2017**, *10*, 894–902.
- [23] L. C. P. Gonçalves, H. R. Mansouri Khosravi, S. PourMehdi, M. Abdellah, B. S. Fadiga, E. Bastos, J. Sa, M. Mihovilovic, F. Rudroff, *Catal. Sci. Technol.* **2019**, *9*, 2682–2688.
- [24] A. Taglieber, F. Schulz, F. Hollman, M. Rusek, M. T. Reetz, *ChemBioChem* **2008**, *9*, 565–572.
- [25] L. Assil-Companiononi, S. Schmidt, P. Heideringer, H. Schwab, R. Kourist, *ChemSusChem* **2019**, *12*, 2361–2365.
- [26] S. Böhmer, K. Köninger, Á. Gómez-Baraibar, S. Bojarra, C. Mügge, S. Schmidt, M. M. M. Nowaczyk, R. Kourist, *Catalysts* **2017**, *7*, 240.
- [27] K. Köninger, Á. Gómez Baraibar, C. Mügge, C. E. Paul, F. Hollmann, M. M. Nowaczyk, R. Kourist, *Angew. Chem. Int. Ed.* **2016**, *55*, 5582–5585; *Angew. Chem.* **2016**, *128*, 5672.
- [28] A. Hoschek, B. Bühler, A. Schmid, *Angew. Chem. Int. Ed.* **2017**, *56*,

COMMUNICATION

- 15146–15149; *Angew. Chem.* **2017**, *129*, 15343–15346.
- [29] A. Hoschek, A. Schmid, B. Bühler, *ChemCatChem* **2018**, *10*, 5366–5371.
- [30] H. Qiang, A. Richmond, Y. Zarni, *Eur. J. Physiol.* **1998**, *33*, 165–171.
- [31] Y. Honda, H. Hagiwara, S. Ida, T. Ishihara, *Angew. Chem. Int. Ed.* **2016**, *55*, 8045–8048; *Angew. Chem.* **2016**, *128*, 8177–8180.
- [32] J. H. Park, S. H. Lee, G. S. Cha, D. S. Choi, D. H. Nam, J. H. Lee, J. K. Lee, C. H. Yun, K. J. Jeong, C. B. Park, *Angew. Chem. Int. Ed.* **2015**, *54*, 969–973; *Angew. Chem.* **2014**, *127*, 983–987.
- [33] S. F. Rowe, G. Le Gall, E. V. Ainsworth, J. A. Davies, C. W. J. Lockwood, L. Shi, A. Elliston, I. N. Roberts, K. W. Waldron, D. J. Richardson, et al., *ACS Catal.* **2017**, *7*, 7558–7566.
- [34] C. Gally, B. M. Nestl, B. Hauer, *Angew. Chem. Int. Ed.* **2015**, *54*, 12952–12956; *Angew. Chem.* **2015**, *127*, 13144–13148.
- [35] J. M. Halder, B. M. Nestl, B. Hauer, *ChemCatChem* **2018**, *10*, 178–182.
- [36] R. E. Parales, K. Lee, S. M. Resnick, H. Jiang, D. J. Lessner, D. T. Gibson, *J. Bacteriol.* **2000**, *182*, 1641–1649.
- [37] C. J. Seel, A. Králík, M. Hacker, A. Frank, B. König, T. Gulder, *ChemCatChem* **2018**, *10*, 3960–3963.
- [38] W. J. Ferguson, K. I. Braunschweiler, W. R. Braunschweiler, J. R. Smith, J. Justin McCormick, C. C. Wasmann, N. P. Jarvi, D. H. Bell, N. E. Good, *Anal. Biochem.* **1980**, *104*, 300–310.
- [39] C. M. H. Ferreira, I. S. S. Pinto, E. V. Soares, H. M. V. M. Soares, *RSC Adv.* **2015**, *5*, 30989–31003.
- [40] D. Adam, L. Bosche, L. Castaneda-Losada, M. Winkler, P. Apfel, T. Happe, *ChemSusChem* **2017**, *10*, 894–902.
- [41] S. Langer, M. Hashimoto, B. Hobl, T. Mathes, M. Mack, *J. Bacteriol.* **2013**, *195*, 4037–4045.
- [42] Y. Suzuki, N. Koyama, *Biodegradation* **2009**, *20*, 39–44.
- [43] C. G. Hatchard, C. A. Parker, *Proc. R. Soc. London. Ser. A. Math. Phys. Sci.* **1956**, *235*, 1203, 518–536.
- [44] R. Yamanaka, K. Nakamura, M. Murakami, A. Murakami, *Tetrahedron Lett.* **2015**, *56*, 1089–1091.
- [45] K. Nakamura, R. Yamanaka, *Tetrahedron: Asymmetry* **2002**, *13*, 2529–2533.

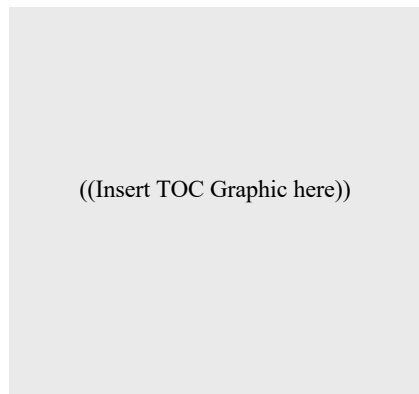
COMMUNICATION

Entry for the Table of Contents (Please choose one layout)

Layout 1:

COMMUNICATION

Text for Table of Contents



Author(s), Corresponding Author(s)*

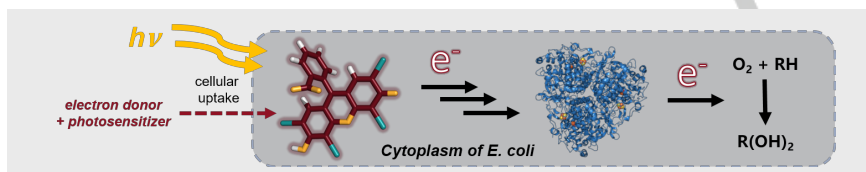
Page No. – Page No.

Title

((Insert TOC Graphic here))

Layout 2:

COMMUNICATION



F. Feyza Özgen, Michael E. Runda, Peter Wied, Bastien O. Burek, Jonathan Z. Bloh, Robert Kourist and Sandy Schmidt*

Page No. – Page No.

Artificial light-harvesting complexes enable Rieske oxygenase-catalyzed hydroxylations in non-photosynthetic cells

Illuminate me! The photo-activation of Rieske dioxygenases in the absence of glucose or any cofactor was successfully conducted using several photosensitizers for the bioconversion of three different substrates and hence represents the first example of a photo-induced Rieske system.